MRS Advances © 2018 Materials Research Society
DOI: 10.1557/adv.2018.436

Controlling donor crystallinity and phase separation in bulk heterojunction solar cells by the introduction of orthogonal solvent additives

Shahidul Alam[1,2], Rico Meitzner[1,2], Christian Kaestner[3], Christoph Ulbricht[5], Stephanie Hoeppener[1,4], Daniel A.M. Egbe[5], Ulrich S. Schubert[1,2], Harald Hoppe[1,2]

[1]*Laboratory of Organic and Macromolecular Chemistry (IOMC), Friedrich Schiller University Jena, Humboldstrasse 10, 07743 Jena, Germany*

[2]*Center for Energy and Environmental Chemistry Jena (CEEC Jena), Friedrich Schiller University Jena, Philosophenweg 7a, 07743 Jena, Germany*

[3]*Institute of Thermodynamics and Fluid Mechanics, Technische Universität Ilmenau, Am Helmholtzring 1, 98693 Ilmenau, Germany*

[4]*Jena Centre for Soft Matter (JCSM), Friedrich Schiller University Jena Philosophenweg 7, 07743 Jena, Germany*

[5]*Institute of Polymeric Materials and Testing, Johannes Kepler University, Altenbergerstrasse 69, 4040 Linz, Austria*

ABSTRACT

The bulk heterojunction morphology of organic solar cells widely controls their device efficiency and stability. Structural order and domain size of the donor phase strongly impact the charge separation efficiency, recombination rates, and the hole percolation through the bulk to the electrode. Herewith, we report a comprehensive study on the control of polymeric order already initiated in solution by the introduction of orthogonal solvent additives to the common solution of anthracene containing poly(p-phenylene-ethynylene)-alt-poly(p-phenylene-vinylene) (PPE-PPV) copolymer, bearing statistically substituted linear octyloxy and 2-ethylhexyloxy side-chains in 1:1 ratio along the backbone (AnE-PVstat), and fullerene derivative phenyl-C61-butyric acid methyl ester (PCBM). The first solvent, a 1:1 blend of chlorobenzene and chloroform, had been discovered to promote phase separation in solution and deposited films. This effect could be further enhanced and was precisely controlled by addition of methanol to the common solution in various volume fractions. Thus the ability to transfer the polymer aggregates from the solution into films was applied to solar cells and is investigated in detail.

Corresponding Author: Shahidul Alam, E-mail: shahidul.alam@uni-jena.de

INTRODUCTION

Organic electronics remains an active area of research and development, mainly due to the potential low-cost production[1],[2],[3], flexibility[4],[5] or semi-transparency[6],[7]. Firstly, applications in modern science, e.g. organic light emitting diodes (OLED) and field effect transistors (OFET)[8], recently more exciting products such as OLED TVs and smartphone displays[9] prove the research success on organic semiconductors over the last decades, and give rise for future application in organic photovoltaics (OPV). Fortunately, the power conversion efficiency (PCE) lately exceeded 11%[10], making this vision closer to reach. One key driver of the solar cell device performance is the morphology of the photoactive layer. The development of the BHJ concept[11],[12], i.e. the introduction of a molecular acceptor to the donor polymer to overcome the exciton binding energy and to facilitate the ultra-fast electron transfer from the donor polymer to the acceptor fullerene[13],[14],[15], paved the way to intense studies on the control of morphology of donor:acceptor blends, among the ongoing development of more efficient molecular donor and acceptor materials[16],[17],[18],[19]. Since the charge separation of excitons is taking place at the interface of polymer and fullerene, an intimate mixture, and hence a large interfacial area, of both materials improves the charge separation efficiency of photo-generated excitons[13],[14],[20]. Unfortunately, also the recombination rate increases as the charge percolation is limited within the homogeneously intermixed phases[21]. Pristine phase separated polymer domains may impede the charge generation due to the loss of interfacial area, but improve the hole transport, which is additionally influenced by the degree of structural order within the polymer phase[21],[22],[23],[24], i.e. π–π-stacking on the short-range and crystallinity on the long-range[25],[26],[27],[28], and its purity[29]. The electron percolation itself is comparably high within the fullerene phase, which mostly forms structurally ordered aggregates[30],[31]. In general, fullerene aggregation is beneficial for charge separation due to the multitude of energy levels present for charge transfer[32],[33],[34]. Thus, larger scale phase separation between the polymer and fullerene improves the charge separation and extraction from the bulk but leads to a loss of interfacial area and the number of free charges. Furthermore, crystallization of pristine phases leads to narrowing of their specific HOMO-LUMO-gap, the energetic distance between the highest occupied molecular orbital (HOMO) and the lowest unoccupied molecular orbital (LUMO). While charge separation is improved within the intermixed phases, the charge recombination is impeded within the more ordered transport phases due to energy relaxation from the intermixed charge generation phases into the crystalline charge transport phases[35],[36],[37],[38]. Hence a proper domain size of phase separated bulk materials is inevitable since the photo-generated excitons within the pristine bulk material have to reach the interface between the polymer and fullerene for dissociation. The exciton lifetime and thus the diffusion length of about 10–20 nm is limited[39],[40].

There exists an optimum for the blend morphology, which consists of finely intermixed domains for efficient charge generation and more extensive scale phase separated domains for efficient charge extraction and minimization of recombination events. Adequately adjusted blend morphologies thus yield an energy landscape, where photo-generated charge carriers are relaxing from finely intermixed higher energy domains towards higher ordered, and lower energy phase separated domains in which they can be efficiently transported to the electrodes. This constellation further discourages charge carriers from energetically uphill recombination, giving rise to the often observed Langevin pre-factors in the range of 10^{-4}. Yielding such morphology is relying on different aspects of materials organization, in which a good part is based on finding a proper mode for aggregation of organic semiconductors within the final

photoactive layer or blend film. Conclusively, fine-tuned blend morphology is required to maximize charge generation and minimize charge recombination as well as improved charge transport and extraction. Several approaches have been studied to enhance polymer crystallization and phase separation from the fullerene, e.g. post-processing like solvent and thermal annealing[41],[42], use of solvent blends and additives[43],[44],[45] with orthogonal solubility of polymer and fullerene and strongly differing vapor pressure, slow drying[46], or preprocessing like polymer aggregation in solution via thermal annealing and introduction of orthogonal-solvents[47],[48],[49],[50],[51]. The resulting degree of polymer aggregation and phase separation from the fullerene can be fast and easily determined from absorption and emission spectroscopy.

In the present work, we studied the influence of an orthogonal solvent, added to the pristine polymer solution, on the aggregation of the semi-crystalline copolymer AnE-PV*stat*, which is the best performing polymer of the AnE-PV class so far[52],[53],[54],[55]. Structural order of the polymer in solution was investigated by UV-vis spectroscopy. Structural order and phase separation within deposited films of AnE-PV*stat*:PCBM blends were studied by absorption and photoluminescence (PL) spectroscopy as well as atomic force microscopy (AFM). The structural data were then related to the hole mobility and photovoltaic parameters, obtained from space-charge-limited-current (SCLC) and solar cell devices respectively, to conclude about the relationship between morphology and the device performance.

EXPERIMENTAL

Polymer:PCBM solutions were prepared from mixtures of semi-crystalline AnE-PV*stat* and PCBM. The synthesis of AnE-PV*stat* is described elsewhere[52]. PCBM was used as received from the supplier Solenne. The chemical structures of AnE-PV*stat* and PCBM are sketched in **Figure 1**.

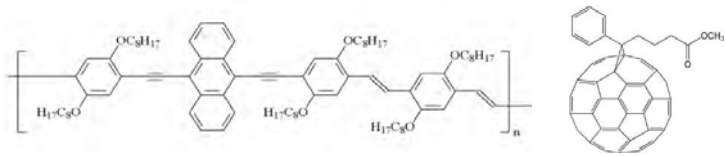

Figure 1: Chemical structure of AnE-PV*stat* (left) and PCBM (right).

The global polymer:PCBM weight ratio was held constant at 2:3 as found to be the AnE-PV*stat*:PCBM ratio with optimal polymer aggregation and phase separation from PCBM[55]. AnE-PV*stat* and PCBM were dissolved in a 1:1 blend of chlorobenzene (CB):chloroform (CF) as found to be the optimal mixture promoting phase separation in AnE-PV:PCBM blends[56]. To control and further investigate the crystallization and phase separation process of the polymer, 5 vol.-% methanol (Sigma-Adrich) was added to the common solution.

Thin films of AnE-PV*stat*:PCBM blends were spin cast on glass substrates for absorption and photoluminescence (PL) spectroscopy measurements. Solar cell device preparation on glass involved pre-structured ITO-layer for selective contacting of the back electrode, followed by spin coating of PEDOT:PSS (Clevios PH, Heraeus). PEDOT:PSS films were then annealed at 170°C for 15 minutes to release residual moisture and were immediately transferred to a nitrogen-filled glovebox. The top aluminum electrode was deposited by physical vapor deposition. Space charge limited current (SCLC) devices for hole mobility measurements were prepared with the organic

layer deposited under the same conditions as for solar cell fabrication. The selective injection of the desired charge carriers was achieved by tuning the work function of the contacts near the HOMO level of the donor material (hole-only device). Therefore, molybdenum trioxide (MoO_3) with a work function of about 6.6 eV was used as bottom injecting contact for holes and top blocking contact for electrons, which was finalized with silver on top, both using physical vapor deposition.

UV-vis spectra of solutions were recorded with a SPECORD 250 ANALYTIC JENA AG spectrophotometer. Thin film steady-state photoluminescence (PL) spectra were recorded with an Avantes AvaSpec ULS-2048 fiber spectrometer. PL excitation was performed with a laser diode emitting at 405 nm. For PL normalization thin film transmission and reflection spectra were recorded with two Avantes AvaSpec-ULS3648-USB2-UA-25 fiber spectrometers simultaneously and reassembled to the thin film absorption spectra. Surface topography measurements were performed in tapping mode on a NTEGRA Aura (NT-MDT) using tapping mode cantilevers from Mikromasch (NSC35). Current-voltage (I-V) characteristics of solar cells and SCLC devices were recorded with a computer controlled source measure unit Keithley 2400 under one sun AM1.5 illumination with a class A solar simulator (SolarLight, XPS 400) and in the dark, respectively. The dark current-voltage characteristics were fitted by using Murgatroyd´s formula[57].

$$I = \frac{9}{8}\varepsilon_0\varepsilon_r\mu_h exp\{0.89\gamma\sqrt{F}\}$$

I is the hole current, μ_h the hole mobility without field dependence, ε_r the relative permittivity of AnE-PV*stat*:PCBM blend (ε_{PCBM} = 3.9[58] and $\varepsilon_{AnE\text{-}PVstat}$= 3.6), ε_0 the vacuum permittivity, γ the field activation factor, L the active layer thickness (~270nm) and $F = V/L$ the average electric field across the active layer, where V is the applied potential.

Electroluminescence (EL) spectra were recorded with an AvaSpec ULS-2048 fiber spectrometer in a home built setup. A Keithley 2601 source measure unit was used for excitation of the samples with a100 mA injection current under forwarding bias.

RESULTS AND DISCUSSION

In order to gain information about the impact of adding an orthogonal solvent to the AnE-PV*stat* polymer solutions based on mixed chlorobenzene (CB):chloroform (CF) solution, transmittance spectroscopy was applied. Hence an original 1 ml AnE-PV*stat* solution was continously diluted with 1 ml methanol, leading to an apparent drop in absorption strength. However, no oscillator strength was lost, and a further effective reduction in total integrated absorption directly corresponded to precipitation of polymer aggregates from solution. **Figure 2** displays the derived optical absorption spectra of AnE-PV*stat* in solution. Upon step-wise addition of the orthogonal solvent (methanol), a new absorption peak at ~600 nm is detected, which has to be associated with the formation of AnE-PV*stat* aggregates. Along with this “binding state,” also a small blue shift for the formerly main absorption peak is visible, relating to the “anti-binding state” of the molecular aggregate.

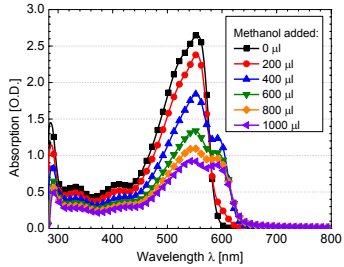

Figure 2: Change in absorption spectra of 1 ml AnE-PV*stat* in CB:CF solution upon addition of up to 1 ml methanol to the pristine polymer solution in various volume fractions.

Thin films of AnE-PV*stat*:PCBM blends on glass substrates were processed from solutions at room temperature under nitrogen atmosphere and were subdued spectroscopic and morphological studies. The obtained absorption and normalized PL (corrected for absorption at the excitation wavelength) spectra are shown in **Figure 3**. By the addition of only 5 vol.-% methanol to the solution, the absorption strength is somewhat increased under normal incidence in comparison with the pristine blend solution. It seems that the polymer is gaining more absorption over the fullerene peak located at about 330 nm, thus hinting to a more substantial fraction of parallely oriented polymer chains with respect to the substrate. Significant changes in the ratio of the transition bands, $A_{0\text{-}0}$ (at 540 nm) and $A_{0\text{-}1}$ (at 580 nm), are not present, which means that there is no noticeable change in the inter-chain order of the polymer due to the addition of methanol[55]. However, the inter-chain order is generally large in semi-crystalline AnE-PV*stat*[25] films.

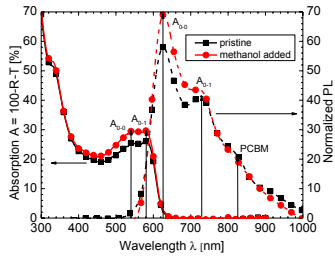

Figure 3: Thin film absorption and photoluminescence spectra of AnE-PV*stat*:PCBM films (pristine and 5 vol.-% methanol added). PL spectra are normalized to the thin film absorption at 405 nm laser excitation wavelength.

In order to compare the PL intensities between the thin film samples, the recorded PL spectra have been normalized/corrected with respect to the absorption at the excitation wavelength (405 nm) of the laser. Higher total polymer PL intensity is observed in case of methanol which is added to the solution. This can be related to extended phase separation or larger polymer domains, which is in good agreement with the development of aggregates which is found already in solution (or during drying of the film)[55].

To gain further insight into the morphology, especially phase separation and domain sizes, of the blend system, tapping mode AFM measurements were performed on

the same samples that were used for optical characterization. The obtained topography and phase images of 2.5×2.5 µm² scans of the blend films are shown in **Figure 4**. The addition of methanol to the solution resulted in larger domains evolved at the surface of the film. It can be derived that also larger domains must be within the film, as the drying process is generally too fast to evolve different scales of phase separation throughout the thin film. The observation of larger domains whether they are pristine polymer or not is in good agreement with the increased polymer PL intensity. The AFM images suggest that in films cast from solutions with methanol additive the PCBM is segregated to the free surface, moreover in PCBM-loaded films, the PCBM nanoclusters are also covered by another polymer "skin" layer[59],[60],[61]. It is further interesting to note that in case of the methanol modified blend casting, a vivid substructure in the phase image hints to a fibrillary organization of the polymer[62]within the larger domains – a good agreement with higher aggregation of the polymer from solution.

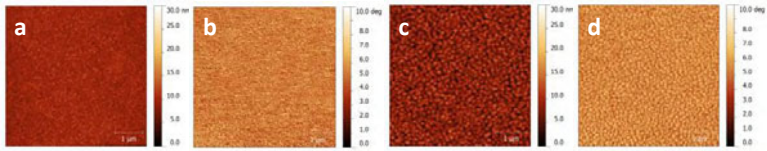

Figure 4: Tapping mode 2.5×2.5 µm² topography (a and c) and phase (b and d) images of AnE-PV*stat*:PCBM blend thin film (pristine (a and b) and 5 vol.-% methanol added (c and d)).

To gain insight into the impact of crystallinity and phase separation in the blend of optoelectronic properties of the bulk-heterojunction, solar cells were fabricated with and without the addition of 5 vol.-% methanol to the solution. The dark and light current density-voltage (*J-V*) characteristics are shown in **Figure 5.** The photovoltaic parameters are depicted in **Table 1.**

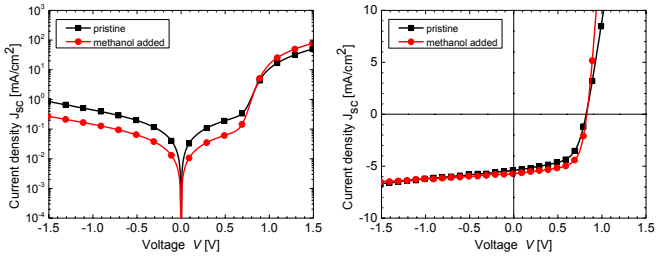

Figure 5: Current density-voltage (*J-V*) characteristics of AnE-PV*stat*:PCBM solar cells. Left: under dark and right: under one sun illumination.

Table 1: Photovoltaic parameters of the AnE-PV*stat*:PCBM solar cells fabricated without and with methanol as a solvent additive.

Sample	J_{sc} (mA/cm^2)	J_{sc}_EQE (mA/cm^2)	V_{oc} (mV)	FF (%)	PCE (%)	PCE_EQE (%)	R_s (ohm)	R_p (ohm)
pristine	5.39	5.85	819	59	2.59	2.83	35	2274
methanol added	5.71	6.16	825	65	3.08	3.31	13	2868

From dark *J-V* characteristics, it is obvious that in case of the methanol modified solution the resulting devices exhibit a better blocking behavior, respectively a more considerable parallel resistance (R_p), and a higher rectification. Both factors generally contribute to an improved performance under illumination, which is indeed detected. Whilst the open circuit voltage stays virtually the same, just bearing a slight increase for the modified blend, the parallel resistance substantially increased and the series resistance (R_s) decreased. This decrease already hints to an improved charge transport, which is further supported by the increased fill factor (FF). A higher FF is generally a sign of an improved mobility-lifetime product of the charge carriers, which can be associated with improved phase separation, as already indicated by the PL measurements. In addition, an increase in R_p may be related to an improvement in vertical phase alignment, and a decrease in R_s hints to the same but also to an improved charge transport capability. Both findings are indeed in line with the increased fill factor. Finally, it is interesting to note that the short circuit photocurrent also enhanced slightly, which demonstrates that the improved charge transport properties are not compromised with a too large phase separation as found earlier[55].

External quantum efficiency (EQE) spectra were recorded with bias light of about one sun on the same samples, shown in **Figure 6**. Indeed, the EQE spectra confirmed the short-circuit current densities obtained from the *J-V* characteristics. The calculated short-circuit current densities, derived from the spectral response of the EQE measurements, are shown in the inset of the graph. Interestingly, the EQE signal of films casted from methanol added solution is increased in the region of 320 nm to 480 nm, which is dominated by PCBM. This may hint to the somewhat improved exploitation of the PCBM contribution to the overall absorption, which can be expected in case of more even distribution over the film thickness[29, 63] (also compare with similar effects for lateral arrangements[64]). However, the contribution of the polymer to the photocurrent seems unchanged in the active layers deposited from solutions with methanol additive, indicating that the polymer phase separation is on its limit and domains should have an optimal size.

To get a deeper insight into the interfacial characteristics, electroluminescence (EL) spectra were recorded from the solar cells under a forward current of 100 mA (corresponding to a current density of about 238 mA/cm²). The EL spectra are depicted in **Figure 6** right. Here, the ratio of the single transitions, especially the polymer emission (peaking at ~ 630 nm) and the charge transfer emission (peaking at 920-950 nm), is relevant[65]. A dramatic increase of the charge transfer (CT) emission (around 800 nm to 1100 nm) is observed, compared to the polymer emission (around 560 nm to 730 nm). This indicates improved access to the interfacial area between polymer and PCBM by charge carriers – most probably via improved percolation and thus charge transport within more ordered phases. This can be, connected to an improved vertical alignment of the materials within the photoactive layer, as already indicated by the increased parallel resistance, leading to a more efficient injection and transport of holes and electrons from the anode and cathode, respectively, towards the materials interface at the heterojunction. It is furthermore interesting to note that the peak energy of the CT-transition seems to be reduced (from ~920 to ~ 945 nm) for the methanol modified blend, which confirms a higher order in the transport states[65], respectively the access to them during charge injection – and vice versa, charge extraction.

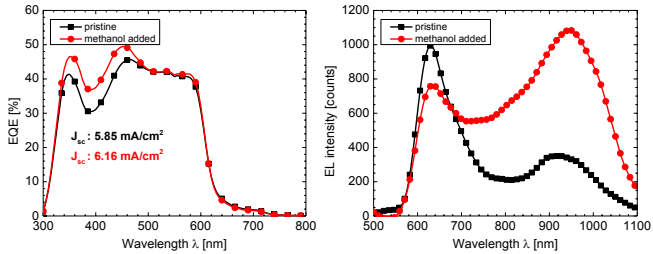

Figure 6: EQE (left) and EL (right) characteristics of AnE-PV*stat*:PCBM solar cell.

Having pointed out a possible increase in charge carrier mobility, specifically for the holes as these are transported within the potentially better-ordered domains of the aggregated polymer, hole-only space-charge-limited-current (SCLC) devices were to be investigated for validation. The charge carrier hole mobility was evaluated by fitting the dark current density-voltage using Murgatroyd's formula. The results are depicted in **Figure 7.** Indeed the methanol modified blend films exhibit a 50% increase in hole mobility, which in good agreement with the improved fill factor. This improvement in mobility has to be related to an enhancing molecular ordering of the polymer and the enhanced phase separation in the blend[66], when methanol is introduced into the solution.

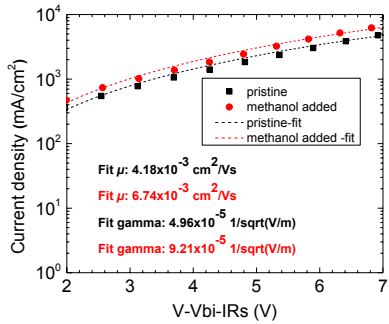

Figure 7: SCLC of hole-only devices prepared from pristine solution and after addition of methanol additive.

An earlier work, demonstrated that methanol added in much smaller quantities might have a positive effect on various polymer:fullerene blends[67]. Not only the addition of methanol to the solution improved the photovoltaic performance, but also top-casting of methanol onto the dry film of the active layer or even the PEDOT:PSS layer. However, polymer aggregation was not accounted for in that study, and as the addition to the solution was one order of magnitude smaller, different effects or mechanisms may be active there. In our research – using a substantially higher methanol concentration – aggregation of the polymer was forced already in solution. This aggregation could be successfully transferred into active layers, leading to an increase of phase separation, whilst keeping the charge generation at the same level. Favorable vertical phase alignment was concluded from photovoltaic and electroluminescence

characterizations, and higher order within the polymer domains from optical spectroscopy. The latter was furthermore confirmed by the AFM measurements. Whilst in the present study the performance was limited by the current generation due to the shortcomings of the polymer batch, this approach can be transferred to other – higher performing – material systems.

CONCLUSION

The orthogonal or anti-solvent additive induced aggregation of the polymer donor in solution could be successfully transferred into blend films in organic photovoltaic bulk heterojunctions. Although this is indeed not the first time applying this method, we believe to have shed more light into the effects of charge generation, transport and selective extraction, which is partly derived from the improved charge injection and recombination from electroluminescence measurements. It could be shown that the introduction of methanol additive to the common solution led to more substantial and better-ordered polymer domains and a more dispersed PCBM phase, which was furthermore confirmed by the 50% increase in hole mobility. In summary, these morphological improvements resulted in an enhanced charge generation, transport, and extraction as well as an impeded recombination of free charges, leading to an overall increase of all solar cell parameters. It is expected that similar strategies can be applied to much better performing solution processed donor-acceptor systems – without modification of the molecular structure.

ACKNOWLEDGMENTS

SA and HH are grateful for financial support from Deutsche Forschungsgemeinschaft(DFG) in the frame of “PhotoGenOrder” project. C. Ulbricht and D. A. M. Egbe thank FWF for research funding through grant No : I 1703-N20. D. A. M. Egbe also acknowledges funding from the SOLPOL project(www.solpol.at).

REFERENCES

[1] S. E. Shaheen, D. S. Ginley, and G. E. Jabbour, MRS Bulletin **30**, 10 (2005).
[2] E. Ahlswede *et al.*, Applied Physics Letters **92**, 143307 (2008).
[3] S.-I. Na *et al.*, Solar Energy Materials and Solar Cells **94**, 1333 (2010).
[4] T. T. Larsen-Olsen *et al.*, Advanced Energy Materials **2**, 1091 (2012).
[5] F. C. Krebs *et al.*, Solar Energy Materials and Solar Cells **93**, 422 (2009).
[6] G. M. Ng *et al.*, Applied Physics Letters **90** (2007).
[7] D. Han *et al.*, Optics Express **18**, A513 (2010).
[8] http://www.printedelectronicsworld.com/. (Access 13th December 2017)
[9] www.oled-info.com/, (Access 13th December 2017).
[10] M. A. Green *et al.*, Progress in Photovoltaics: Research and Applications **25**, 3 (2017).
[11] N. S. Sariciftci *et al.*, Synthetic Metals **59**, 333 (1993).
[12] G. Yu *et al.*, Science **270**, 1789 (1995).
[13] N. S. Sariciftci *et al.*, Science **258**, 1474 (1992).
[14] B. Kraabel *et al.*, Chemical Physics Letters **213**, 389 (1993).
[15] R. A. J. Janssen *et al.*, Journal of Chemical Physics **103**, 788 (1995).
[16] C. B. Nielsen *et al.*, Accounts of Chemical Research **48**, 2803 (2015).
[17] J.-S. Wu *et al.*, Chemical Society Reviews **44**, 1113 (2015).
[18] I. Etxebarria, J. Ajuria, and R. Pacios, Organic Electronics **19**, 34 (2015).

[19] C. Liu *et al.*, Chemical Society Reviews **45**, 4825 (2016).
[20] N. E. Jackson *et al.*, J. Phys. Chem. Lett. **6**, 77 (2015).
[21] A. Pivrikas *et al.*, Progress in Photovoltaics: Research and Applications **15**, 677 (2007).
[22] M. T. Dang *et al.*, Chemical Reviews **113**, 3734 (2013).
[23] C. R. Singh *et al.*, Journal of Polymer Science Part B: Polymer Physics **51**, 943 (2013).
[24] D. T. Duong *et al.*, Advanced Functional Materials **24**, 4515 (2014).
[25] S. Rathgeber *et al.*, Macromolecules **43**, 306 (2010).
[26] S. Rathgeber *et al.*, Polymer **52**, 3819 (2011).
[27] E. J. W. Crossland *et al.*, Advanced Materials **24**, 839 (2012).
[28] R. Noriega *et al.*, Nat Mater **12**, 1038 (2013).
[29] C. Kastner *et al.*, Proc. SPIE **9184**, 91840Z (7 pp.) (2014).
[30] C. Waldauf *et al.*, Advanced Materials **15**, 2084 (2003).
[31] T. B. Singh *et al.*, Organic Electronics **6**, 105 (2005).
[32] B. M. Savoie *et al.*, J. Am. Chem. Soc. **136**, 2876 (2014).
[33] S. Gélinas *et al.*, Science **343**, 512 (2014).
[34] F. C. Jamieson *et al.*, Chem. Sci. **3**, 485 (2012).
[35] J. Nelson, Materials Today **14**, 462 (2011).
[36] M. A. Brady, G. M. Su, and M. L. Chabinyc, Soft Matter **7**, 11065 (2011).
[37] F. Liu *et al.*, Journal of Polymer Science Part B: Polymer Physics **50**, 1018 (2012).
[38] N. D. Treat, and M. L. Chabinyc, in *Annual Review of Physical Chemistry, Vol 65*, edited by M. A. Johnson, and T. J. Martinez (Annual Reviews, Palo Alto, 2014), pp. 59.
[39] S. M. Menke, and R. J. Holmes, Energy & Environmental Science **7**, 499 (2014).
[40] I.-W. Hwang, D. Moses, and A. J. Heeger, The Journal of Physical Chemistry C **112**, 4350 (2008).
[41] F. Padinger, R. S. Rittberger, and N. S. Sariciftci, Advanced Functional Materials **13**, 85 (2003).
[42] W. Ma *et al.*, Advanced Functional Materials **15**, 1617 (2005).
[43] E.-C. Chen *et al.*, Applied Physics Letters **92**, 1 (2008).
[44] J. K. Lee *et al.*, Journal of the American Chemical Society **130**, 3619 (2008).
[45] Y. Yao *et al.*, Advanced Functional Materials **18**, 1783 (2008).
[46] G. Li *et al.*, Nat Mater **4**, 864 (2005).
[47] N. Kiriy *et al.*, Nano Letters **3**, 707 (2003).
[48] W. Y. Huang *et al.*, Macromolecules **41**, 7485 (2008).
[49] A. J. Moulé, and K. Meerholz, Advanced Materials **20**, 240 (2008).
[50] S. Sun *et al.*, Journal of Materials Chemistry **21**, 377 (2011).
[51] H. Yan *et al.*, The Journal of Physical Chemistry C **115**, 3257 (2011).
[52] D. A. M. Egbe *et al.*, Journal of Materials Chemistry **20**, 9726 (2010).
[53] Ö. Usluer *et al.*, Journal of Polymer Science Part A: Polymer Chemistry **50**, 3425 (2012).
[54] C. Kästner *et al.*, Journal of Polymer Science Part B: Polymer Physics **50**, 1562 (2012).
[55] C. Kastner, D. A. M. Egbe, and H. Hoppe, Journal of Materials Chemistry A **3**, 395 (2015).
[56] C. Kastner *et al.*, Journal of Polymer Science Part B-Polymer Physics **51**, 868 (2013).
[57] P. N. Murgatroyd, Journal of Physics D: Applied Physics **3**, 151 (1970).
[58] V. D. Mihailetchi *et al.*, Advanced Functional Materials **13**, 43 (2003).
[59] H. Hoppe *et al.*, Adv. Funct. Mater. **14**, 1005 (2004).
[60] H. Hoppe *et al.*, Mol. Cryst. Liquid Cryst. **426**, 255 (2005).
[61] H. Hoppe, and N. S. Sariciftci, J. Mater. Chem. **16**, 45 (2006).
[62] C. Kastner *et al.*, Journal of Materials Chemistry **22**, 15987 (2012).
[63] H. Mangold *et al.*, Physical Chemistry Chemical Physics **16**, 20329 (2014).
[64] S. Engmann *et al.*, Synthetic Metals **161**, 2540 (2012).
[65] C. Kästner *et al.*, Advanced Science **4**, 1600331, 1600331 (2017).
[66] C. Kästner *et al.*, 2014), pp. 91840Z.
[67] O. Synooka *et al.*, Adv. Energy Mater. **4**, 10 (2014).